

Received 25 April 2022, accepted 3 August 2022, date of publication 10 August 2022, date of current version 18 August 2022.

Digital Object Identifier 10.1109/ACCESS.2022.3197877

RESEARCH ARTICLE

Joint Mobile Node Participation and Multihop Routing for Emerging Open Radio-Based Intelligent Transportation System

SEPEHR ASHTARI¹, (Graduate Student Member, IEEE),

MEHRAN ABOLHASAN¹, (Senior Member, IEEE),

JUSTIN LIPMAN^{1,2}, (Senior Member, IEEE), NEGIN SHARIATI^{1,2}, (Senior Member, IEEE),

WEI NI³, (Senior Member, IEEE), AND ABBAS JAMALIPOUR⁴, (Fellow, IEEE)

¹Faculty of Engineering and IT, University of Technology Sydney, Ultimo, NSW 2007, Australia

²Food Agility CRC Ltd., Ultimo, NSW 2007, Australia

³The Commonwealth Scientific and Industrial Research Organization (CSIRO), Sydney, NSW 2122, Australia

⁴Faculty of Engineering, The University of Sydney, Sydney, NSW 2006, Australia

Corresponding author: Sepehr Ashtari (sepehr.ashtarinakhaei@student.uts.edu.au)

ABSTRACT This paper proposes joint mobile node participation and routing protocol for multi-hop device-to-device (MD2D) networking in intelligent transportation systems, called fuzzy-based participation and routing protocol for MD2D (FPRM). Our proposed protocol is designed to operate over future open-radio access networks (O-RANs). We introduce a sub-layer at the network layer that can determine nodes with the highest participation probability in routing using a fuzzy logic system, thus building a framework to create more stable routes. To ensure the participating nodes are capable of handling the data traffic, two constraints are proposed, mobility and coverage constraints. The former enables the creation of sustainable communication links, and the latter enforces the communication service to the entire MD2D network. Simulation results show that our approach can increase the network lifetime, decrease the end-to-end (E2E) delay, and increase the packet delivery ratio (PDR) compared to the existing proactive routing protocol. Our protocol outperforms the benchmarked MD2D protocols and other investigated ad hoc protocols.

INDEX TERMS MD2D communication, routing protocol, fuzzy logic system, network automation, O-RAN, AODV, OLSR, HSAW.

I. INTRODUCTION

The widespread use of mobile devices, intelligent transportation systems, Internet-of-things (IoT) networks, and machine-type communication has led to substantial data traffic growth. This trend will most likely continue as the need for ubiquitous connectivity of people, devices, and machines follow the same trajectory. In this trend, mobile devices have significantly contributed due to advancements in new applications and services for smartphones. These applications require high data rates and perfect quality of experience (QoE) for users. The need for a faster data rate was the primary reason for wireless network evolution and the manifestation of fifth-generation (5G) cellular networks. However,

with the emergence of smart applications [1], the Internet-of-everything (IoE) [2], user demands [3], and the connection of millions of people, machines, and vehicles [4], the current network paradigm requires shifting from rate-centric to ultra-reliable low latency communication. Therefore, creating an unprecedented dispute for existing 5G wireless networks. The sixth-generation (6G) cellular network is expected to overcome many associated issues in 5G by utilizing intelligence and a new radio access network (RAN) [5]. Although one can argue that available 5G systems in the market can handle basic IoE and low latency services, it is disputable whether they can deliver tomorrow's heterogeneity of innovative city applications.

Significant effort has been dedicated to enhancing the RAN architecture [6]. The goal is to build an operator-defined RAN on open hardware that enables intelligent radio control and

The associate editor coordinating the review of this manuscript and approving it for publication was Hassan Omar¹.

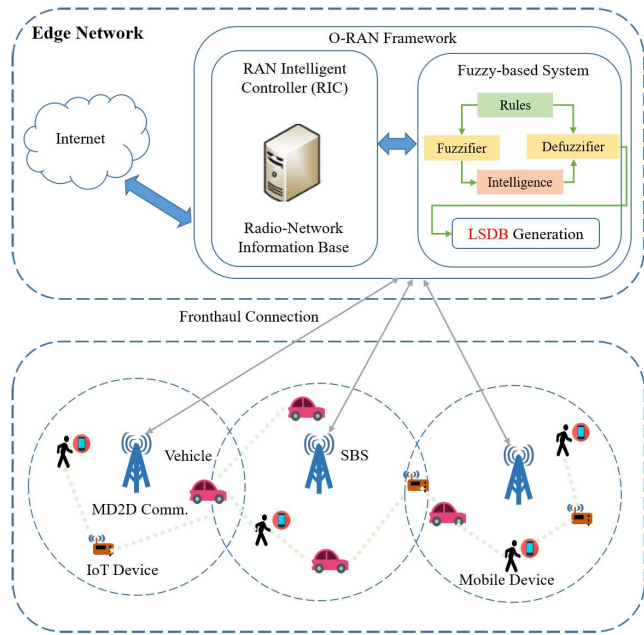


FIGURE 1. Proposed framework for the designed routing protocol, where fuzzy-logic system is adapted in O-RAN intelligent controller.

creates self-driving networks. In particular, the open-radio access network (O-RAN) allows openness in the RAN by merging the xRAN forum and centralized-RAN alliance. O-RAN uses the concept of virtualization, cloud, and intelligence to initiate agile service deliveries and enhance capabilities to end users [7]. Incorporating intelligence is one of the main reasons underlying the advantages of 6G over 5G. 6G establishes an automation and self-organization network, where most network applications will be ruled by a machine rather than human intervention. One of the main building blocks in 6G is machine learning (ML) technology [8]. ML has significantly contributed to wireless network applications, such as quality-of-service (QoS), resource management, spectrum allocation, and routing [9]–[12]. Moreover, software-defined networking (SDN) enables the separation of control and data planes, allowing ML-based algorithms to perform optimization and automation in a centralized controller and provide intelligent decisions to devices. SDN and network functions virtualization (NFV) provide advanced features for the RAN intelligent controller (RIC) to increase the performance of future wireless networks. Furthermore, O-RAN has defined three control loops, effectively enabling NFV applications to be deployed at different locations of the cellular network architecture. For example, at the core, where the non-real-time control loop exists, non-real NFV applications could be deployed, whereas, in the near-real-time control loop, NFVs aim to perform operations at near-real-time [13], [14].

A. MOTIVATIONS

Multi-hop device-to-device (MD2D) communication is a promising technology to offload base station (BS) traffic.

In MD2D frameworks, routing algorithms play an essential role, and they must be designed to provide the highest performance based on the criteria of the current and future networks. Therefore, an MD2D routing protocol must be capable of adapting to any dynamic topology changes in the network. Recent MD2D routing protocols mainly focus on optimization algorithms to increase network performance. To the best of our knowledge, no MD2D study has yet adapted a fuzzy-based topology control routing mechanism to identify the participant nodes and dynamically create efficient routes for that specific network topology. One of the advantages of our proposed framework is the intelligence of controller. The controller can collect network telemetry and network application requirements and use them to generate link-state databases (LSDBs). Moreover, the topology control mechanism enables a fuzzy system to dynamically adapt to the network changes and identify the participating nodes. Our routing protocol can create network knowledge and prescribe optimal routes using the information obtained from the topology control and acquired data from the network.

B. CONTRIBUTIONS

This paper proposes an intelligent joint topology control and multi-hop routing called fuzzy-based participation and routing protocol for MD2D (FPRM) to increase the network lifetime and packet delivery ratio (PDR). In our approach, a fuzzy-based participation mechanism controls and manipulates the network's topology. The fuzzy system is located in the RIC controller. The controller collects all the nodes' information and decides whether a node should participate in MD2D routing based on the fuzzy rules. Therefore, different network graphs can be obtained by manipulating which node can participate in the network. Based on the topology graphs and application requirements, network LSDBs are created. Figure 1 represents the fuzzy-based participation and routing framework under the management and control of the O-RAN framework. In this framework, every small BS (SBS) (e.g., picocell networks) is connected to a RIC controller with a unique ID, and every BS can communicate to other SBSs through backhaul channels. Each SBS is responsible for providing service to every user equipment (UE) in their coverage area. The edge network is connected to the core network for Internet access and other advance processing functionalities. RIC creates a centralized fuzzy-based unit to process and store information to instruct the SBSs. The embedded fuzzy system obtains the participating nodes and creates different network LSDBs based on the network topology and application requirements. Later the LSDB is shared with participating nodes to perform MD2D routing.

The contributions of this paper are summarized as follows:

- Proposing joint topology control and MD2D routing using an adaptive fuzzy-based learning system.
- Presenting a new MD2D knowledge-based routing framework that adapts based on the user requirements and fuzzy system to identify participating nodes and

disregard nodes that can cause potential damage to network performance.

- Utilizing an intelligent O-RAN controller to collect network information and build various LSDBs for different network topologies.
- Introducing a three-step routing constraint to ensure the proposed MD2D routing can provide a reliable communication link to the maximum number of users over a long time.
- A comprehensive analysis of the proposed routing protocol with a semi-centralized routing protocol, namely hybrid SDN architecture for wireless distributed networks (HSAW) [15], and traditional distributed routing protocols, including ad hoc on-demand distance vector (AODV) and optimized link state routing (OLSR), is presented. The results show more than a 30% increase in average throughput, more than 30% reduction in end-to-end (E2E) delay, almost 8% increase in PDR, and almost 2% decrease in energy consumption compared to one of the leading MD2D routing protocols, HSAW.

The rest of this paper is organized as follows. Section II provides a literature review of the current MD2D routing protocols. Section III briefly explains the routing framework and system model. Section IV describes the route discovery and maintenance strategy over an intelligent fuzzy-based routing protocol. Section V provides a complete explanation of the fuzzy logic algorithm used for node participation. Section VI introduces the constraint used after the fuzzy logic process to improve the scalability of the routing protocol. Section VII evaluates the performance of the proposed routing framework using the NS-3 simulator. Finally, our conclusion and future research directions are explained in Section VIII.

II. RELATED WORKS

The O-RAN provides the opportunity to create a new generation of intelligent semi-centralized routing protocols [16], [17]. This opportunity has opened the door toward developing a new set of MD2D routing protocols for future intelligent transportation systems. In MD2D routing, a controller can instruct the devices in the network and install or remove routing entries within the device's routing tables. For instance, the authors in [18] proposed a routing protocol using the SDN framework in the wireless multi-hop paradigm to increase the life span of the network. In their framework, nodes transmit their local information to the controller to generate a global network view. The SDN controller can then provide a route to a destination upon request from a source node. This is generally achieved by computing the shortest route via the shortest path first (SPF) algorithm. The SDN controller applies energy constraints and hops count limits to find the best path for each source node. The simulation results show that the network lifetime is extended compared to OLSR and AODV routing protocols. Authors of [19] proposed an MD2D routing protocol for SDN-based cellular networks. The proposed method builds the LSDB of the network at the controller, and once a

node requests a route, the controller uses the Dijkstra algorithm to find the shortest path to the destination. The proposed protocol provides scalability and reliability in mobile ad hoc networks (MANETs). Furthermore, in vehicular ad hoc networks (VANETs), the authors of [20] proposed a low delay and low routing overhead framework to propagate messages. Their protocol finds multiple paths using multiple network attributes, such as link stability and shortest travel time. Simulation results show that the proposed protocol significantly outperforms the conventional routing protocols regarding E2E delay and routing overhead. SDN-based routing frameworks provide scalable routing procedures among various wireless networks. However, the above strategies have not considered the dynamic changes of the network causing deterioration of network performance. One of the promising solutions to address this problem is using O-RAN near-real-time controller to make routing decisions. Fuzzy-based routing protocols have shown promising solutions for optimization of routing parameters in a self-organizing manner based on the network dynamics [21].

Recently, knowledge-based algorithms have gained widespread attention. The optimized data acquired from SDN-enabled ML-based controller can create knowledge that enables networks to adjust their parameters when necessary [22]–[24]. For instance, the authors of [25] used reinforcement learning (RL) in routing problems to maximize the throughput and minimize the communication delay for each source node. Their algorithm continuously predicts the network's future behavior and evaluates the most efficient path to the destination. An SDN controller is utilized to collect network information and train an RL agent to manage the data traffic among devices in the network. Simulation results illustrate that the proposed routing protocol delivers large files faster than open shortest path first (OSPF) and least loaded (LL) routing algorithms over different network scenarios. Moreover, the authors of [26] proposed an intelligent-based fuzzy routing protocol to decrease power consumption. Specifically, they solved the unbalanced distribution of cluster heads by the fuzzy c-means clustering algorithm, which categorized nodes into balanced clusters. Then the cluster heads are assigned using the Mamdani fuzzy inference system to route packets between the controller and other nodes. Obtained simulation results show an increase in network lifetime and superiority over existing clustering-based protocols. Other studies, such as [27], used fuzzy logic to improve the stability of the AODV routing protocol in MANETs. The most trusted relay nodes are selected in their framework for route generation between the source and destination nodes. The fuzzy logic method takes the node energy, mobility, and hop counts to determine the node trust level. The simulation results illustrate the proposed framework's advantages against AODV in terms of control overhead, network throughput, packet delivery ratio, and E2E delay. In vehicular networks, fuzzy learning has provided unprecedented benefits. The authors of [28] introduced an intelligent fuzzy-based routing scheme for software-defined

vehicular networks (SDVNs) in urban areas. In this technique, a centralized controller maintains the routing table. These routing tables are initially constructed based on the priorities of packets using fuzzy logic and later updated based on the network changes. Then, a greedy strategy is used to obtain routing paths with the highest link stability. Simulation results demonstrate significant performance improvement in dense urban areas compared to the existing routing frameworks. As can be seen from the literature review, the ability to learn and adjust the network parameters to increase the network performance is a promising solution for future MD2D heterogeneous networks [29]–[31].

III. SYSTEM MODEL

FPRM is a proactive routing protocol where a controller collects the network information and broadcasts the required routing information for participant nodes to perform MD2D communication. In general, the controller is responsible for separating the control and data planes such that the distributed devices only transmit the data messages, not the control messages. When the controller is adapted in the network, devices are relieved from flooding algorithms to find a route to the destination. The controller is responsible for creating paths separately and only providing devices with routing entries. Proactive routing protocols use the capability of a centralized controller to build LSDBs. However, the generated LSDB is shared with the entire network without knowing whether devices are participating in the MD2D routing or not. This can cause cellular channel overhead and reduction in the MD2D network lifetime. To mitigate problems associated with proactive routing approaches and increase the network's lifetime, we are introducing a sub-layer, which can determine nodes with the highest participation probability in routing and thus build a framework to create more stable routes.

As shown in Figure 2 the O-RAN-enabled BS collects every node's data, such as energy, number of neighboring nodes, and mobility rate, to obtain the most reliable nodes. The fuzzy system processes the information and defines the participating nodes. Furthermore, the controller creates an LSDB and broadcasts it to the participating nodes, where nodes will distributively calculate a path using the LSDB. Once a node requires to transmit a packet, it will evaluate the path using Dijkstra's algorithm and adds the route to its routing table. If a link failure occurs while sending the packet, the node can calculate a new route and delete the previous route from the routing table. Additionally, the link failure is shared with the controller, where the controller updates the fuzzy system and broadcasts the new information to nodes to update their LSDBs.

In our framework, every UE is equipped with at least two communication interfaces: cellular/licensed and WiFi/unlicensed frequencies for in-band and out-band communication. The in-band communication consists of data messages exchanged between UEs (MD2D communication) and the acknowledgment messages. Out-band communication includes Internet connectivity, control messages, and

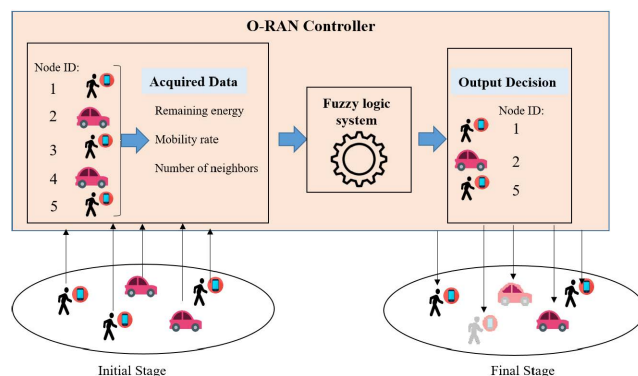


FIGURE 2. Proposed fuzzy framework, where nodes information including remaining energy, mobility rate, and the number of neighboring nodes are collected by the controller to apply fuzzy system and identify the participating nodes.

connection to other networks. At the initial stage of the network, each UE transmits a Hello message to its neighboring nodes (where neighboring nodes are nodes within each UEs communication range) via the WiFi channel. Then, UEs transmit their link-state information to the sub-controller via the cellular channel. Based on the received data, the sub-controller processes the information and generates an LSDB. Then, fuzzy logic is applied to find the participation policy in the network. The sub-controller uses defined fuzzy rules to calculate each node's eligibility index (EI). The lowest values of the EI correspond to nodes that might fail to transmit a packet or have low energy levels. These nodes are excluded from participation in routing. Moreover, once the eligible node is determined, the next step is applying the following constraints: coverage and mobility. The introduced constraints in our proposed routing framework ensure that the eligible/active nodes can support the entire network with the least interruption. It is noteworthy that The LSDB is only transmitted to active nodes in the network.

IV. ROUTING PROCEDURE IN FUZZY-BASED MD2D COMMUNICATION FRAMEWORK

At the initial stage of our framework, nodes transmit their information, such as remaining energy, list of neighboring nodes, mobility rate, and throughput. Once the BS receives all this information, it will run them through the fuzzy logic system to obtain nodes with the least EI. These nodes are in critical conditions, and using them in the routing process may cause packet loss leading to an unstable network. After selecting eligible nodes, the next step is to compute each node's activation time duration. Then, we apply mobility and coverage constraints to enforce two rules: first, least interrupted connectivity, and second, providing service to the entire network. Then, the active nodes will receive the computed LSDB from the BS.

A. LSDB CALCULATION

The controller provides the entire network with link-state information, calculated in a centralized manner using the

weight given to each node. The link-state information contains the reported data of nodes, including a list of neighboring nodes, the traffic arrival rate, the queue length of each node, and the channel condition between the node and the one-hop neighboring nodes. To compute the LSDB, once a node joins a BS after the authentication process by the sub-controller, it will be allowed for advance routing services. Then, each node will broadcast its existence through Hello messages to its neighboring nodes via a WiFi channel. After the adjacent nodes are identified and the link between them is established, each node will send its link-state information via the cellular channel to the sub-controller. This information consists of one-hop neighboring nodes associated with link-state, location, battery level, and throughput and sent to the BS using a topology control (TC) message. The LSDB generated at the sub-controller is also shared with the nearby sub-controllers and the main controller. Therefore, each BS has a global network view, helping them with handover decisions, traffic management, user allocation, and content caching.

B. LSDB UPDATE

Each sub-controller must update the generated LSDB after any changes to the network. If any changes occur to the link-state information, a TC message will be sent to the sub-controller to inform the status changes of the node. Based on the TC message, the sub-controller decides whether to change the LSDB. The new information received at the BS is processed to update the main LSDB and broadcast any link state changes. Moreover, if any node observes sudden changes and failure to the link, the BS is notified, and new LSDB entries are generated based on the information. The proposed algorithm only updates specific entries of the node's LSDB. However, the entire LSDB is usually updated at a constant rate.

C. ROUTE DISCOVERY

Our fuzzy-based routing framework is a hop-by-hop routing protocol, meaning that the data packets only carry the node destination ID. Each intermediate node or active node between the source and destination is the relay node. The relay nodes are the forwarding devices that check the destination field ID and then apply Dijkstra's algorithm to discover the next forwarding node. Each forwarding device has the entire network LSDB enabling them to find the least-cost path to the destination. After receiving LSDB, an active node performs distributed route discovery using Dijkstra's algorithm [32]. In particular, each node generates a routing table that specifies a path to any other node in the network with minimum total cost. In this stage, no further assistance is required from the controller. Nodes are now able to perform route discovery purely in a distributed manner. Multiple routes can be established between any two nodes as primary and backup routes based on the lowest cost in case of any link breakage. If both paths are independent, the data traffic can be split between the two routes to deliver the packet in

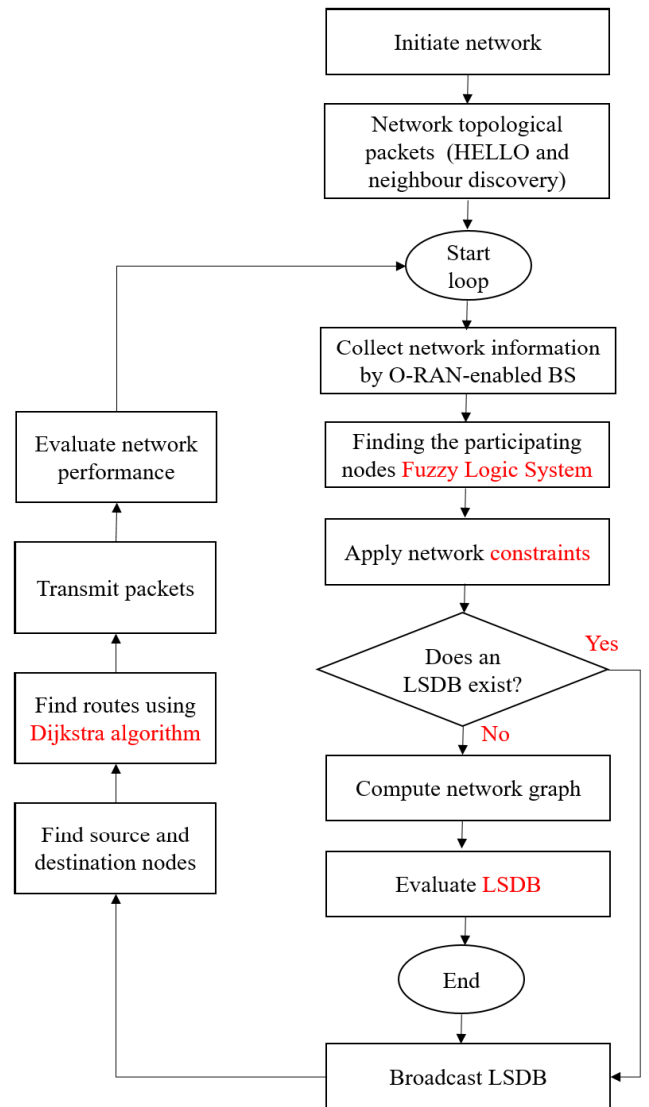


FIGURE 3. Flowchart of the proposed fuzzy-based routing protocol.

parallel. In the case of heavily congested networks with a high number of nodes, route discovery is more challenging, and split multipath routing helps distribute the load. On the other hand, if multiple paths are stored in each node for any pairs of nodes, then node storage and network scalability will be another challenge. To further accomplish scalability, we can deploy sub-controllers and divide the network into small cells similar to the idea in [33] and [34]. Hence, each node only needs to maintain the routing table of its own cluster. However, this is the point of our future study to monitor the effect of split routing in congested networks.

D. ROUTE MAINTENANCE

Each relay node is responsible for forwarding packets to the next least-cost hop. After any reception, relay nodes must acknowledge the packet delivery. If a node detects a failure or error during transmission, it will initiate a flow error (FERR) message to the sub-controller containing the error type. If the

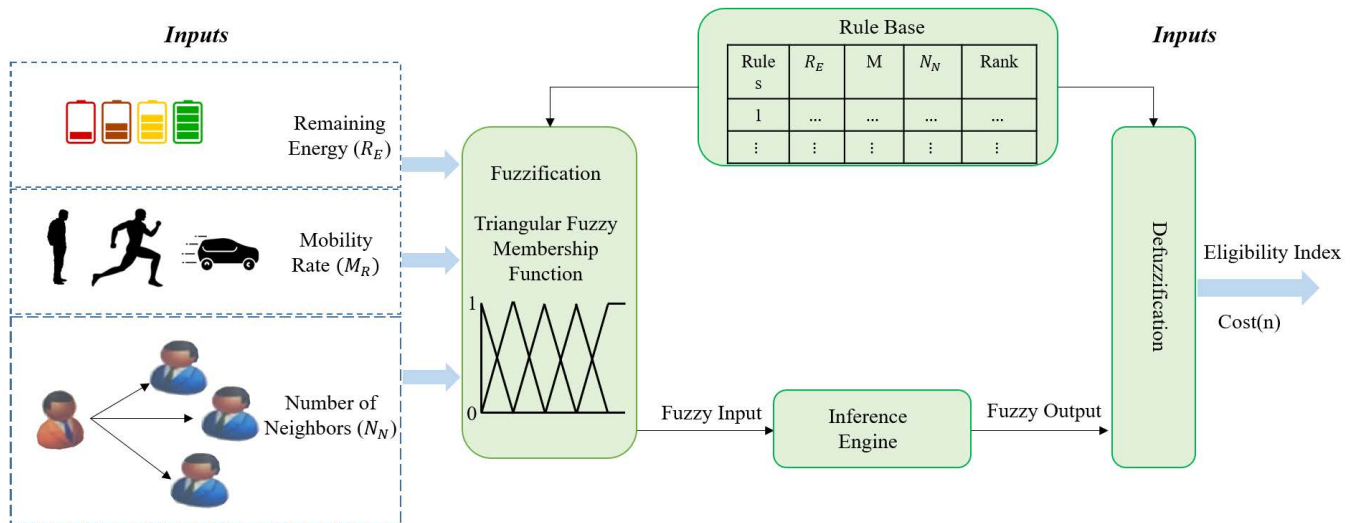


FIGURE 4. The proposed fuzzy system.

error type has the link broken message, the sub-controller broadcast a FERR to notify other nodes about the broken link. Once nodes receive a FERR from the BS, any transmission to that particular node will be canceled, and the node ID is removed from the LSDB after the flow error waiting time (FERR-WT) period. FERR-WT is the associated time for deleting any entry and updating the LSDB. This time duration is required if the node is only deactivated for a short period due to bad reception. After this time is passed and nodes have not yet received an active route entry, a new route will be obtained, and the routing table will be updated. At the same time, the previous node of the forwarding path uses the LSDB and applies Dijkstra's algorithm to find the alternative path and transmit the rest of the data packet using the new route. During the route failure, nodes can find a new path due to the availability of the LSDB. However, if a new path can not be found, then there are two possibilities:

- Destination is unreachable: If the node can not find a destination, the sub-controller will receive a destination ID with the data packet.
- Low channel quality: In this case, the sender transmits a quality check message to the receiver to check the possibility of transmission. If not, a new route will be established.

1) OVERVIEW

In parallel to LSDB computation, the BS is also responsible for obtaining the eligible nodes through a fuzzy system. Figure 3 shows the overall process of the proposed protocol and all the required steps to compute the participating nodes and the routes. A fuzzy system is equipped with rules and can evaluate the eligible nodes. After the fuzzy system is applied, the three-step constraint is performed to ensure the eligible nodes computed by the fuzzy system are satisfactory if any specific condition occurs. Then, LSDB is shared among the eligible nodes, and the MD2D communication is established

between the active flows. The following section explains how nodes are segregated into two groups: active and deactivated nodes—followed by applying constraints for the final eligibility check.

V. NODE PARTICIPATION MECHANISM USING FUZZY-BASED ALGORITHM

The main idea of fuzzy logic is to manage a system with pre-defined rules. The results of fuzzy logic consist of values ranging from 0 to 1. There are four main procedures in fuzzy logic: fuzzification, fuzzy rules, fuzzy inference system, and defuzzification. The fuzzy logic in our study aims to construct the initial stage for the participation of nodes. The fuzzy system captures network information in our framework and computes each node's EI. This index will identify the probability of a node being able to participate in a route.

A. FUZZIFICATION

The fuzzification process measures the node cost (NC) to estimate the node's EI. The cost is calculated using three decision parameters: remaining energy, mobility rate, and the number of neighbors. These parameters are transformed into triangular fuzzy membership functions, where each input value to the system is mapped to the associated membership function to reveal the fuzzy degree. Figure 4 presents the fuzzy logic flowchart.

Figure 5 illustrates the membership diagrams for obtaining the fuzzy value of remaining energy, mobility rate, and the number of neighboring nodes, respectively. The first input parameter to the fuzzy system is the remaining energy of a node. As shown in Figure 5a the membership function consists of five levels, including very low, low, medium, high, and very high. We assume that the energy of nodes is randomly distributed with a maximum value of 300 Joules. The high remaining energy value represents a high-value node, which means that the node with higher remaining energy has

TABLE 1. The proposed fuzzy rules.

Rules	Remaining Energy	Mobility Rate	Number of Neighbors	Rule Cost	Numerical Representation of Cost
1	Very Low	Very High	Very Low	Very Low	0
2	Very Low	Very High	Low	Very Low	0
3	Very Low	Very High	Medium	Very Low	0
4	Very Low	High	Very Low	Low	0.25
5	Very Low	High	Low	Low	0.25
6	Very Low	High	Medium	Low	0.25
7	Very Low	Medium	Very Low	Low	0.25
8	Very Low	Medium	Low	Low	0.25
9	Very Low	Medium	Medium	Low	0.25
10	Low	Very High	Very Low	Very Low	0
11	Low	Very High	Low	Very Low	0
12	Low	Very High	Medium	Very Low	0
13	Low	Medium	Very Low	Very Low	0
14	Low	Medium	Low	Low	0.25
15	Low	Medium	Medium	Low	0.25
16	Low	High	Very Low	Very Low	0
17	Low	High	Low	Very Low	0
18	Low	High	Medium	Very Low	0
19	Medium	Very High	Very Low	Low	0.25
20	Medium	Very High	Low	Low	0.25
21	Medium	Very High	Medium	Low	0.25
22	Medium	High	Very Low	Low	0.25
23	Medium	High	Low	Low	0.25
24	Medium	High	Medium	Low	0.25
25	Medium	Medium	Very Low	Low	0.25
26	Medium	Medium	Low	Medium	0.5
27	Medium	Medium	Medium	Medium	0.5

a low risk of packet transmission failure. The amount of the remaining energy is converted to linguistic values in one or two possible levels.

As shown in Figure 5b the second input parameter is the mobility rate of the nodes. The higher the nodes' mobility, the larger the probability of packet failure is due to link failure or signal fluctuations. Therefore, when the mobility rate of nodes is low, the node's reliability is high, which means there is a better chance of relaying packets to the destination with minimum interruption and packet loss.

Finally, the third input parameter to the fuzzy system is the number of neighbors, as shown in Figure 5c. A node with a higher number of neighbors has a higher connectivity degree and a higher chance of participating in the routing.

B. FUZZY RULES

Fuzzy rules are obtained using the degree of importance and representation of a value into a meaningful explanation. As previously mentioned, the highest node energy is assumed to be 300 Joules, and if, for instance, a node reports an energy level of 270 Joules, the node is still at a very high energy level. As a result, we can assign each input parameter to the fuzzy system to the corresponding linguistic values in a reasonable belief. As illustrated in Figure 5 each parameter, remaining energy, mobility rate, and the number of neighbors are divided into five levels. Therefore, we have three fuzzy parameters leading to 5^3 states. However, there are only 27 rules counted in our system to distinguish the least qualified nodes and eligible nodes for participating in the

routing. These 27 rules are demonstrated in Table 1, where each rule is associated with a cost. The associated cost values will be explained later in this section.

C. FUZZY INFERENCE ENGINE

After the fuzzification process and converting input values to linguistic values, the values are sent to the inference engine. Together with the rules and the input data, the inference engine forms inferences and draws conclusions. The fuzzy inference system considers all the possible states of the applied rules to evaluate the fuzzy inference output. The Mamdani fuzzy inference system [35] is used in this step to find the fuzzy matching rules and calculate the fuzzy inference output. The system's output is sent to the defuzzification module for final processing.

D. DEFUZZIFICATION

In the defuzzification process, the output values of the fuzzy inference engine are used to calculate the crisp value of the EI as a final crisp value of the fuzzy learning system. EI is calculated using (1), where $Rule_i$ is computed via the corresponding values of the x-axis into the y-axis. Rule cost, also known as the cost function, is represented by a triangular function. The numerical representation of rule cost C is obtained using Figure 6.

$$EI(n) = \frac{\sum_{i=1}^n Rule_i C_i}{\sum_{i=1}^n Rule_i} \quad (1)$$

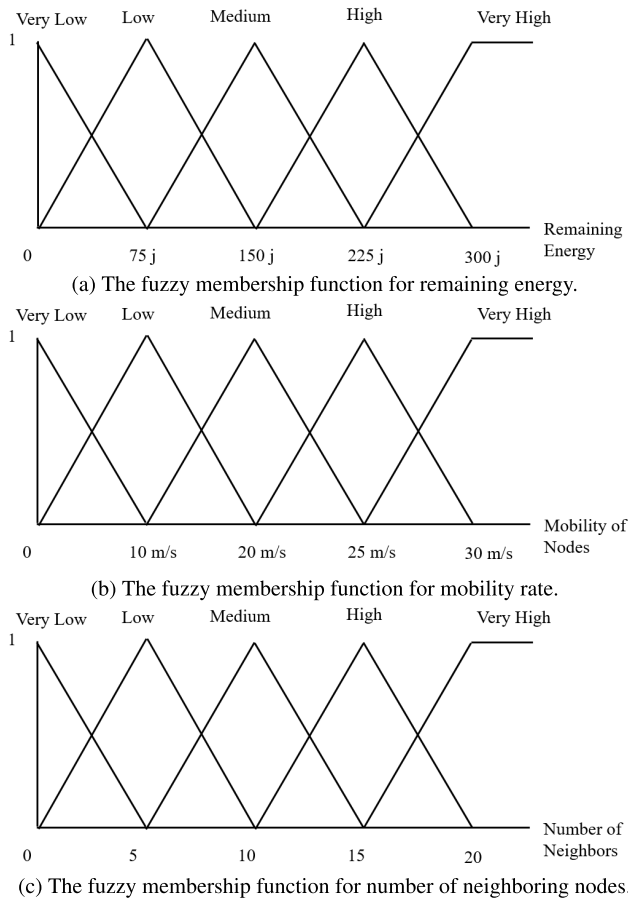


FIGURE 5. Proposed fuzzy diagrams for evaluating the potential candidate for participation.

Note that to calculate the y-values from the fuzzy functions, some values of the x-axis might cross two points in the y-axis. For instance, for the mobility value of 15m/s, the corresponding y-value is 0.5. On the other hand, for the mobility rate of 17m/s, the y-values intersect at two points; the low-line at 0.4 and the medium-line at 0.6. This process increases the number of states while calculating the EI.

Let us consider an example for node A reporting the remaining energy of 125 Joules, mobility rate as 27m/s, and 4 neighboring nodes. Using fuzzy functions these values correspond to: $R_{E(low)} = 0.3$, $R_{E(medium)} = 0.7$, $M_{R(medium)} = 0.4$, $M_{R(high)} = 0.6$, $N_{N(verylow)} = 0.1$, and $N_{N(low)} = 0.9$. Each parameter corresponds to two values, meaning there are $2^3 - 1$ states to calculate rules. Table 2 illustrates the numerical values of rules for each of the states. All three parameters of input (Remaining energy, mobility rate, and the number of neighbors) are now multiplied together. Finally, to compute whether node A can participate, EI is calculated as follows:

$$EI_A = \frac{\sum_{i=1}^n Rule_i C_i}{\sum_{i=1}^n Rule_i} = \frac{Rule_{13} C_{13} + Rule_{14} C_{14} + Rule_{16} C_{16}}{Rule_{13} + Rule_{14} + Rule_{16}}$$

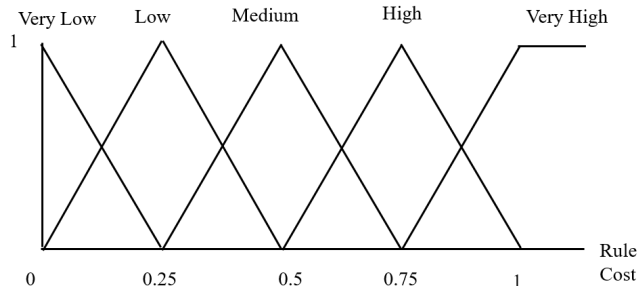


FIGURE 6. Fuzzy diagram for calculating the rule cost of each combined rules from Table 1.

TABLE 2. Numerical representation of rules for provided example to calculate EI.

Rules	Values	Results
$R_{E(low)} \times M_{N(verylow)} \times N_{N(verylow)}$	$0.3 \times 0.4 \times 0.1$	0.012
$R_{E(low)} \times M_{N(verylow)} \times N_{N(low)}$	$0.3 \times 0.4 \times 0.9$	0.108
$R_{E(low)} \times M_{N(high)} \times N_{N(verylow)}$	$0.3 \times 0.6 \times 0.1$	0.018
$R_{E(low)} \times M_{N(high)} \times N_{N(low)}$	$0.3 \times 0.6 \times 0.9$	0.162
$R_{E(verylow)} \times M_{N(verylow)} \times N_{N(verylow)}$	$0.7 \times 0.4 \times 0.1$	0.028
$R_{E(verylow)} \times M_{N(verylow)} \times N_{N(low)}$	$0.7 \times 0.4 \times 0.9$	0.252
$R_{E(verylow)} \times M_{N(high)} \times N_{N(verylow)}$	$0.7 \times 0.6 \times 0.1$	0.042
$R_{E(verylow)} \times M_{N(high)} \times N_{N(low)}$	$0.7 \times 0.6 \times 0.9$	0.378

$$+ \frac{Rule_{17} C_{17} + Rule_{25} C_{25} + Rule_{26} C_{26}}{Rule_{17} + Rule_{25} + Rule_{26}} + \frac{Rule_{22} C_{22} + Rule_{23} C_{23}}{Rule_{22} + Rule_{23}} \quad (2)$$

where logistic values shown in Table 2 represent the rules in Table 1. For instance, the first row in Table 2 corresponds to rule 13 in Table 1. After substituting the values, the EI is 0.26. Similarly, the network’s EI is evaluated, and the lowest values will represent the nodes with the lowest probability of participating in a route. In contrast, the highest values of EI represent nodes with a higher probability of participation. Network constraints will further process the eligible or active nodes to ensure the network’s coverage area is not disturbed and find how long an eligible node can stay active.

VI. APPLIED CONSTRAINTS FOR THE PROPOSED FUZZY-BASED ROUTING FRAMEWORK

In this section, the energy model is first presented, followed by the evaluated active time for the eligible nodes. To ensure all active nodes are capable of providing service to the entire network, a coverage constraint is adopted in our system. Finally, the mobility constraint maximizes the active time and guarantees no transmission failure during activation. After applying the regulations, the final decision on the eligible nodes for participation is made.

A. PROPOSED TIME FRAME FOR NODE PARTICIPATION

In our system, we assume a simple energy dissipation model of radio hardware [36], where the transmitter dissipates energy to send k -bits of packets through a power amplifier and radio electronics, and the receiver dissipates energy to run the received k -bits of a data packet. Then, the energy to transmit the k -bits message is E_{TX} , and E_{RX} is the consumed

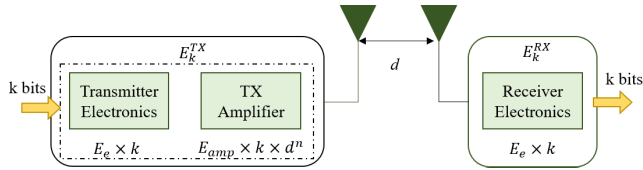


FIGURE 7. Energy consumption model.

energy to capture the message at the receiver. As shown in Figure 7 the energy expenditure to transmit k -bits packet over a distance d is obtained as follows:

$$E_k^{TX} = \begin{cases} E_e k + E_{amp} k d^4, & \text{if } d > d_0; \\ E_e k + E_{fs} k d^2, & \text{if } d < d_0; \end{cases} \quad (3)$$

$$E_k^{RX} = k E_e \quad (4)$$

where d_0 is the threshold distance computed by the $\sqrt{E_{fs}/E_{amp}}$, E_e is the power consumed by the electronic devices, E_{amp} and E_{fs} are the amounts of energy per bit dissipated in the RF amplifier.

Based on (3) and (4), we can approximate that the energy consumed to transmit a packet is almost three times higher than receiving a packet. Considering this fact, let us only consider the highest energy consumption a node can have every second. Assuming that the largest packet size is equivalent to the data rate (R) and distance is less than the threshold, then the maximum consumed energy in every second is equal to:

$$E_{max} = E_e R + E_{fs} R d^2 \quad (5)$$

Moreover, the total energy consumption E_T of the network is evaluated using the number of the packets K sent in every flow $F \in \{1, \dots, f_n\}$ as follows:

$$E_T = \sum_{k=1}^K \sum_{i=1}^F E_{k,i}^{TX} + E_{k,i}^{RX} \quad (6)$$

Having the maximum amount of energy a node might dissipate, we can calculate the maximum time t_{max} a node can stay active. Once the participating nodes are discovered, the next step is to evaluate the time they can remain active. We assume that the activation time duration must not exceed more than the $\alpha\%$ threshold of the initial energy of a node. Based on this assumption, the maximum time a node can stay active can be calculated as follows:

$$t_{max} = \frac{E_{RM} \alpha}{E_{max}} \quad (7)$$

where E_{RM} is the remaining energy of the node. For instance, if we assume the remaining energy of a node is 200j, the data rate of a link is 10Mbps, α is 25%, and assuming the worst case scenario maximum range $d = 100$ (Constants: $E_e = 50nj/bit$, $E_{fs} = 10pj/bit/m^2$, and $E_{amp} = 0.0013pj/bit/m^4$), the maximum time the node can stay active is $t_{max} = 33.33s$.

B. MOBILITY CONSTRAINT

Once the node's maximum activation time t_{max} is calculated, it is a question of whether the node can remain active with

minimum transmission failure considering the neighboring nodes and its own mobility rate. Knowing how fast a node is moving and whether movement might impact the initial coverage area and the number of neighbors is crucial for selecting the best performing node to maximize coverage, capacity, and stability. Therefore, it is essential to declare constraints to determine whether a node can still support its neighbors after a particular movement.

This paper considers a 2-D system with N number of heterogeneous nodes located randomly at positions $[x_i, y_i]^T$, and $i, j \in N$. The distance between each node is defined by their Euclidian distance: $d_{ij} = \sqrt{(x_i - x_j)^2 + (y_i - y_j)^2}$. Each node's maximum transmission area is considered a fixed disk with a given range. All the nodes should be divided into two groups; the first group contains the active nodes, and the second group keeps the temporarily deactivated nodes. Let $K = \{(K_1, w_{k_1}), \dots, (K_m, w_{k_m})\}$ be the set of deactivated nodes, where K_m represents the node ID and w_{k_m} is the corresponding weight to the closest active node. Now let $A = \{(A_1, t_{a_1}), \dots, (A_n, t_{a_n})\}$ be a set of active nodes with the corresponding active time frame. Consequently, based on the maximum activation time, we can derive the final activation time as follows:

$$\sum_{l=1}^L d_{A_l, A_{l+L}} < \max(W_{K_{A_l}}^{A_l}) \quad (8)$$

where L is the number of steps a node will take during the activation time, and $W_{K_{A_l}}^{A_l}$ is the weight of a set of deactivated K_{A_l} nodes allocated to active node A_l . Constraint (8) ensures that the active node is capable of supporting its neighboring nodes or the deactivated nodes in its neighbor (K_m) during the activation time while it is moving.

Along with checking whether the active node movement does not interrupt the communication with neighbors, the movement of K_m must also be monitored for any possible link failures. Z_k is responsible for the movement of K_m , whether the deactivated neighboring node is moving towards or away from the active node A_l .

$$Z_k^i = \frac{d_{A_i, N_j}}{Range} \quad i \in n, j \in m \quad (9)$$

The movement of nodes directly depends on the mobility rate (v). As shown in Figure 8 once nodes start to depart from the initial position, they will move to different indicated areas (shown as rings). Each marked circular ring represents a 20% gap to the initial place, and different transmission ranges represent a different radius. In our study, the transmission range of nodes is limited to 100m. Hence every 20% gap represents a 20m deviation from the initial position. To avoid link failure between neighboring nodes due to movement, the following constraints are established:

$$0 < \max(Z_k^i) < 1, A_i : t_{active} = t_{max} - \frac{t_k}{h}, \quad i \in n \quad (10)$$

$$\max(Z_k^i) \geq 1, A_i : t_{active} = 0, \quad i \in n \quad (11)$$

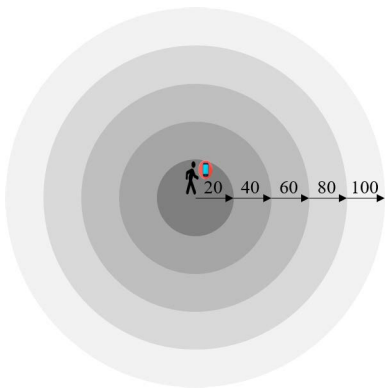


FIGURE 8. Five movement events based on the distance a node can travel over the activation period.

$$t_k = \max(Z_k^i) 100 v_{avg}^K \quad i \in n \quad (12)$$

$$h = \begin{cases} v_{max} \left(\frac{v_{max}}{100}\right)^v & \text{for } 15 < v \leq 30 \\ -\frac{v_{max}}{2} v^2 + v^2 + \frac{v_{max}}{2} & \text{for } 0 \leq v \leq 15; \end{cases} \quad (13)$$

To obtain the activation time (10) is used, where h is evaluated from (13) and v_{max} equals to the maximum mobility rate, assumed to be 30m/s. As shown in Figure 9 if the average node mobility rate is between 0-15m/s, the probability of a node staying active is higher. Therefore, as the average velocity of neighboring nodes (K_m) decreases h -index increases faster to maximize the activation time. However, if the average mobility rate of K_m is greater than 15m/s, the activation time of an active node will decrease dramatically. That means the K_m has a higher chance of leaving the active node’s coverage area. Hence, the activation time will be minimized to ensure packet loss is minimized during any transmission. t_k ensures the active time duration provides the lowest communication link breakages by considering the weight of the furthest K_m and the average node velocity. (11) limits the activation time to ensure deactivated nodes from set K are not out of the transmission range of A . This procedure is conducted at the RIC before finalizing the list of active nodes and allocating the corresponding activation time.

C. COVERAGE CONSTRAINT

Another essential constraint applied in our routing protocol is the coverage constraint to guarantee the initial network coverage by nodes remains almost the same after identifying the active nodes. After active nodes are separated from deactivated nodes, deactivated nodes will not receive the whole LSDB. We can imply that the deactivated nodes are shut down. Hence, the network’s coverage area by all the nodes might be affected when the deactivated nodes are shut down. We introduce a coverage area constraint to solve this problem to keep the final coverage area almost identical to the initial coverage area. In order to formulate the coverage constraint problem a weight (q) is assigned to each node in the network $N = \{(n_i, q_i), \dots, (n_i, q_i)\}$. This weight represents the

strength of the link between two nodes, which means how much overlapping coverage area two nodes might have. The weight of each node is taken as the ratio of the coverage area, a number between 0 and 1.

$$q_{ij} = \frac{A(N_i \cap N_j)}{A(N_i)} \quad (14)$$

If we assume the coverage area of each node follows a disk model with a fixed radius, $A(N_i \cap N_j)$ is the intersection area between the coverage areas of node i and j , where the intersection is computed as follows:

$$A(N_i \cap N_j) = \frac{1}{2} r_i^2 \left[2 \cos^{-1}(\theta_i) - \sin(2 \cos^{-1}(\theta_i)) \right] + \frac{1}{2} r_j^2 \left[2 \cos^{-1}(\theta_j) - \sin(2 \cos^{-1}(\theta_j)) \right] \quad (15)$$

where θ_i and θ_j are defined as follows:

$$\theta_i = \frac{d_{i,j}^2 + r_j^2 - r_i^2}{2 d_{i,j} r_i} \quad (16)$$

$$\theta_j = \frac{d_{i,j}^2 + r_i^2 - r_j^2}{2 d_{i,j} r_j} \quad (17)$$

r_i and r_j are the transmission range of node i and j , respectively. In our simulation, $d_{i,j}$ is the distance between N_i and N_j defined by Euclidean distance. Finally, $A(BS_i) = \pi r_i^2$ is the coverage are of N_i .

Figure 10 provides an example to illustrate the described algorithm. This example presents an area of $10m \times 10m$ with 14 randomly scattered nodes. To calculate the weight of the graph, the weights for all nodes q_i are added.

$$Q_i = \sum_{j \in N} q_{i,j} \quad (18)$$

Based on the weights, nodes are separated into two groups, A' and K' , where A' is the set of nodes that must stay active, and K' is the set of nodes with high Q . That means the list of active nodes found in the previous section must now match with set K' . Then, the list of deactivated nodes must match with online nodes A' to check whether any deactivated node must remain online due to the coverage area restriction. In both cases, the node’s action will be reversed if there is any mismatch. This technique enforces the selected nodes during the fuzzy learning process to be able to provide service to the entire network. In Figure 10 after the weights are all computed, N_2 will have the maximum weight and will be selected as the potential node in set K . If this node is also listed in the fuzzy system deactivated nodes, this node will be selected in the final list of deactivated nodes. Moreover, as observed from Figure 10 the overlapping coverage area of N_1, N_3 and N_7 supports the fact that these nodes are the substitutes in that region, and by coverage constraint, N_2 is part of K' . Similarly, this technique is applied to the entire network to ensure full connectivity.

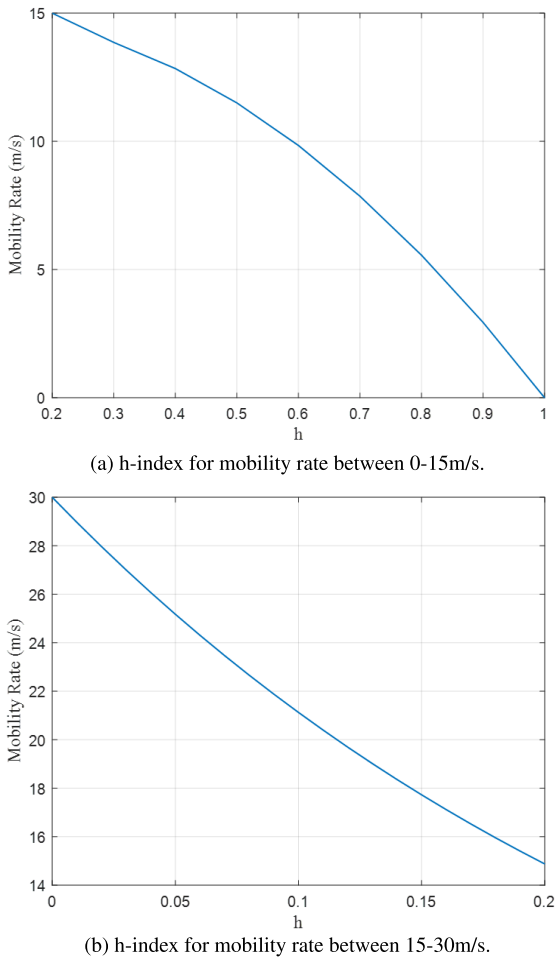


FIGURE 9. h-index for computing the activation time of a node.

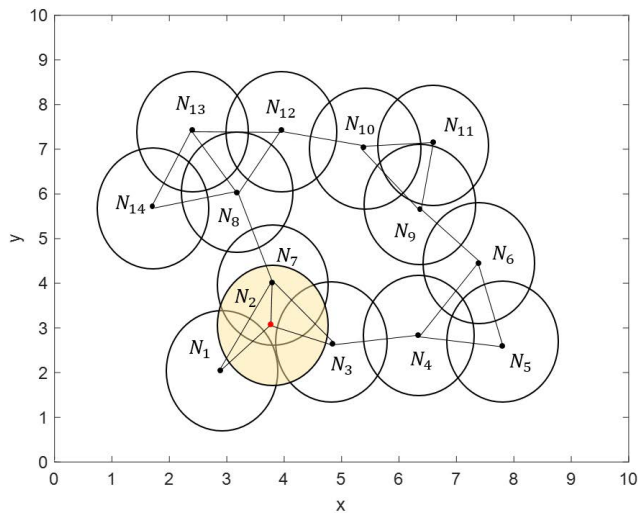


FIGURE 10. A simple illustration of the coverage area of fourteen nodes with their intersections.

VII. SIMULATION RESULTS

This section presents our proposed routing protocol’s simulation setup and performance evaluation. First, the simulation environment with the parameters and assumptions are

TABLE 3. Simulation parameters.

Parameters	Value
Simulation environment	500m × 500m
Number of UEs	50,100,150,200,250
Packet transmission Size	15 kbits
Protocols	FPRM, HSAW, AODV, OLSR
Propagation model	Free space
Mobile node Transmission range	100m
Mobile node movement model	Random waypoint mobility
Total simulation time	3000s

explained. Second, the performance of the proposed routing protocol is thoroughly examined and compared with other routing protocols.

A. SIMULATION SETUP

The proposed FPRM protocol is implemented using the Network Simulator-3 (NS-3). NS-3 simulator supports both IP-based and non-IP-based networks, but we are adapting the IP-based network in our simulation. IP-based simulation in NS-3 involves models for long-term evolution (LTE)/5G, WiFi, worldwide interoperability for microwave access (WiMAX), etc., for layers 1 and 2. This simulator provides different testbeds and protocols for users to run and test their proposed frameworks. For instance, routing problems in MANETs can use protocols such as AODV, OLSR, and dynamic source routing (DSR). NS-3 supports several random mobility generators and also SDN-based networks.

Figure 11 illustrates our simulation environment expanding over a 500m × 500m area. The BS is located in the center of the network. For simplicity, only one network cell is considered with randomly generated nodes between 50 and 250, with 50 nodes increment in every simulation run. Heterogeneous nodes are considered in this simulation, including mobile nodes, IoT devices, and vehicles. However, all the nodes are specified as UE with different mobility rates. Two separate IP-based networks are set for cellular communication and WiFi communication. The cellular communication band is set to apply the LTE/5G specifications using the NS-3 modules. At the same time, the WiFi band is IP-based with IEEE standards. Simulation parameters are shown in Table 3. The simulation results were run for 3000s, and each simulation was averaged over multiple simulations running. We use the Monte Carlo simulation technique under 50 runs to validate our results, and the final results are averaged and plotted with 95% confidence intervals.

B. SIMULATION ANALYSIS

This section provides the simulation results of the proposed fuzzy-based node participation routing using the NS-3 simulator. Three types of nodes with different mobility rates and power are considered to evaluate our proposed routing protocol. First, we assumed that 40% of the network is filled with mobile nodes, 40% with IoT devices, and 20% vehicles. Nodes’ power is randomly distributed between

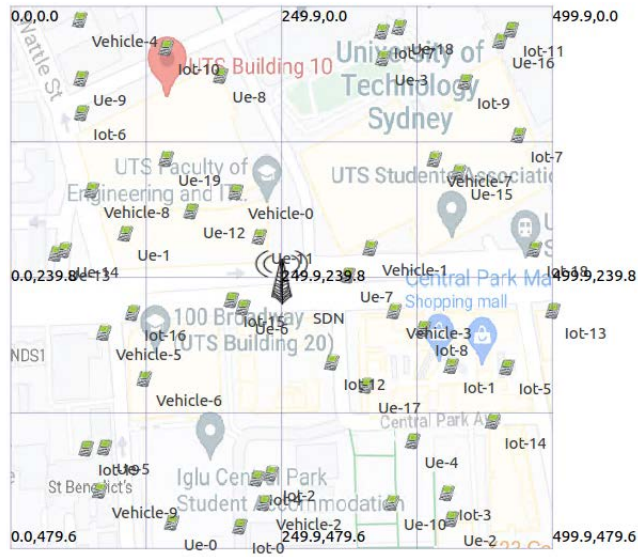


FIGURE 11. Simulation terrain setup.

0-300 joules (the value of power can be changed based on the standards; however, we chose this value to see the impact of depleted nodes). Nodes' velocities are randomly selected between 1-30 m/s. Two channels are considered for data communication, cellular and WiFi. For WiFi or MD2D communication, IEEE802.11n-5GHz is used, and LTE/5G broadcast control channel (BCH) is utilized for cellular communication. We assume that the link quality between nodes is updated every 1 second. In every scenario, the number of active nodes is increased to analyze the performance of the proposed routing protocol. MD2D routing has an average length of 4 hops between any source and destination. We compared our proposed routing framework with our previously proposed routing protocol, HSAW, and two conventional MANET routing protocols: AODV and OLSR. The signal propagation model is Friis free space model [37]. The simulation analysis generates random source and destination nodes. Finally, the assumptions taken during the simulation scenarios are introduced as follows:

- Assuming a random velocity rate from 1-30 m/s second is allocated to each node.
- The network consists of 40% pedestrian, 40% inner-city mobile nodes, and 20% outer-city mobile nodes.
- We consider a simple energy model for our system, randomly distributed among nodes between 0-300 joules per UE. This value is assigned to calculate the amount of consumed energy during the packet transmission process and realize the effect of energy consumption.

This study's main objective is to introduce a new fuzzy-based routing participation protocol to increase the network lifetime, PDR, and throughput. The aim is to use fuzzy logic to identify nodes with the least capabilities to stay deactivated for a specific time. Network constraints are used to check the participant nodes regarding activation time, network coverage, and mobility patterns.

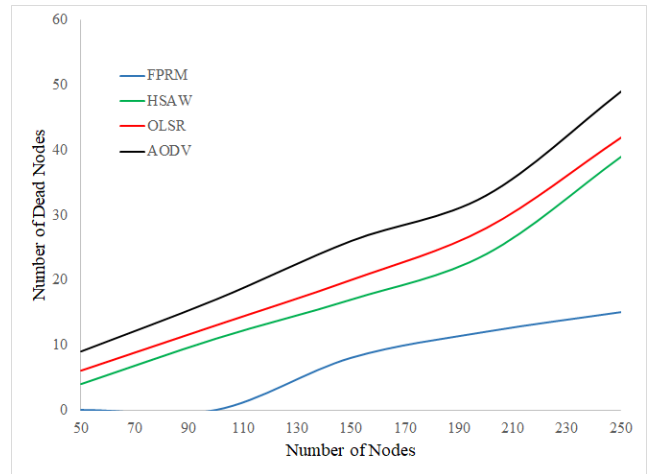


FIGURE 12. Number of depleted nodes.

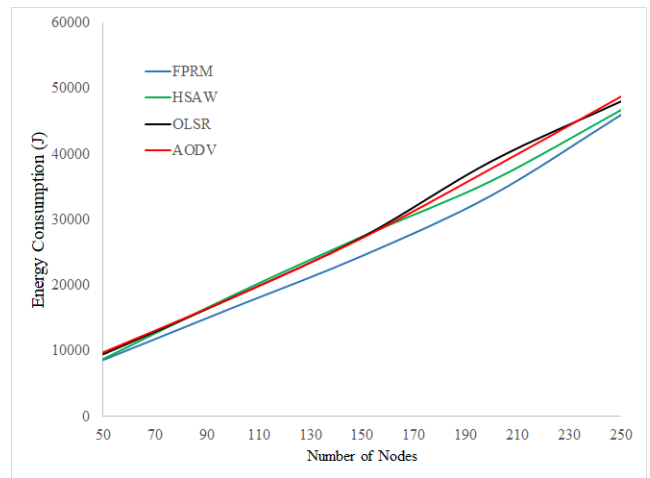


FIGURE 13. Nodes energy consumption.

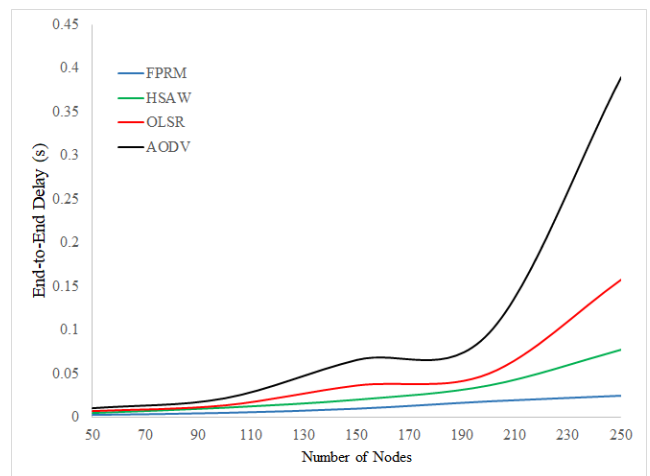


FIGURE 14. End-to-end delay.

Figures 12 and 13 illustrate the number of depleted nodes and the energy consumption, respectively. FPRM shows small improvement over HSAW in network lifetime. There are two reasons why FPRM has a longer lifetime than

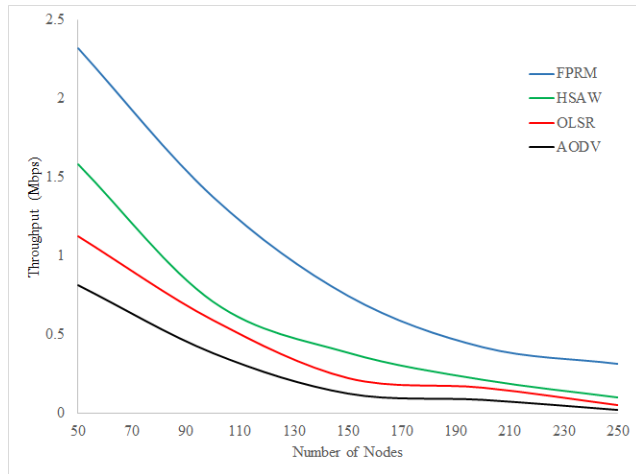


FIGURE 15. Average network throughput.

HSAW and two other conventional routing protocols. First, in HSAW, the entire nodes in the network receive the LSDB, which causes significant energy consumption compared to FPRM. Second, FPRM keeps track of nodes and their energy consumption, and if the energy of nodes passes a certain threshold, the controller stops the node from participating in the routing. FPRM prevents unintentional and unnecessary energy consumption. Therefore, in long-term scenarios, more nodes will be active in the network than in the HSAW. Furthermore, compared to the conventional ad hoc routing protocols, such as AODV and OLSR, FPRM performs much better.

Figure 14 shows the E2E delay of FPRM, HSAW, AODV, and OLSR. FPRM and HSAW perform similarly at low network density, but FPRM accomplishes a better E2E delay once node density increases. In FPRM, nodes have more reliable links because of the active nodes in the network. As described in previous sections, active nodes have maximum energy, lowest mobility rate, and maximum throughput. Therefore, packets are transmitted over more reliable links faster than HSAW. Compared to traditional ad hoc protocols, namely AODV and OLSR, both HSAW and FPRM archive better results. However, FPRM has superior performance overall.

Figure 15 represents the average total throughput of the entire network, including the cellular and MD2D communication channels. Our proposed routing protocol performs significantly better than the three other routing protocols. This is because not all the nodes are active in the network, making the controller use the maximum available throughput. Therefore, the average network throughput increase compared to HSAW, AODV, and OLSR.

Figure 16 shows the PDR of the network, where FPRM achieves significantly higher PDR compared to HSAW, OLSR, and AODV. FPRM has slightly better PDR performance than OLSR and AODV in low-density networks but considerably higher in more congested networks. FPRM has the lowest packet failure due to the fuzzy participation

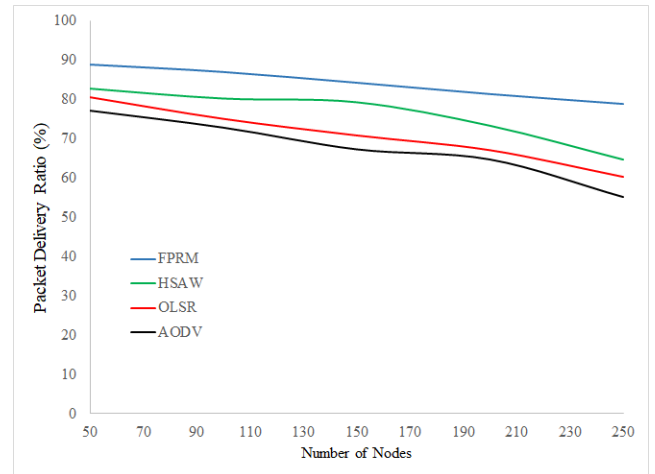


FIGURE 16. Packet delivery ratio.

algorithm. In the participation technique, active nodes are selected based on their performance. Active nodes are responsible for routing the packets, and as long as their performance stays high, the packet dropped will be minimum.

VIII. CONCLUSION

This paper proposed a new joint participation and routing protocol using a fuzzy-based routing framework called FPRM with mobility, energy, and coverage constraints. A new topology control mechanism was presented using the fuzzy-logic-based approach to identify participating nodes and create different network graphs. In our routing protocol, the information collected from the network and application layers are utilized as knowledge in the form of LSDB. In our approach, an O-RAN intelligent controller separates the control plane decision from the data plane. The controller was responsible for creating various LSDBs based on the network information and application requirements. The data plane was only responsible for relaying the data from one end to another. The controller only shares the LSDB with the participating nodes for MD2D routing to reduce cellular channel overhead and energy consumption. Any node with information to transmit is capable of processing the LSDB and obtaining the most efficient route to the destination. The simulation results show that the FPRM protocol is superior in network lifetime, E2E delay, PDR, and throughput than HSAW. Moreover, our protocol significantly improved performance compared to the purely distributed benchmark routing protocols, AODV and OLSR.

This study's future direction is to explore the timing mechanism of how often the topology control update is required to trigger and optimize this time. Moreover, LSDBs can be optimized by machine learning algorithms to contain only a specific form of knowledge based on the topology graphs.

REFERENCES

- [1] L. Zhu, F. R. Yu, Y. Wang, B. Ning, and T. Tang, "Big data analytics in intelligent transportation systems: A survey," *IEEE Trans. Intell. Transp. Syst.*, vol. 20, no. 1, pp. 383–398, Jan. 2018.

- [2] P. Padhi and F. Charrua-Santos, "6G enabled industrial internet of everything: Towards a theoretical framework," *Appl. Syst. Innov.*, vol. 4, no. 1, p. 11, Feb. 2021.
- [3] G. Liu and D. Jiang, "5G: Vision and requirements for mobile communication system towards year 2020," *Chin. J. Eng.*, vol. 2016, pp. 1–8, Apr. 2016.
- [4] Y. Xu, G. Gui, H. Gacanin, and F. Adachi, "A survey on resource allocation for 5G heterogeneous networks: Current research, future trends, and challenges," *IEEE Commun. Surveys Tuts.*, vol. 23, no. 2, pp. 668–695, Sec. 2021.
- [5] L. Bonati, M. Polese, S. D'Oro, S. Basagni, and T. Melodia, "Open, programmable, and virtualized 5G networks: State-of-the-art and the road ahead," *Comput. Netw.*, vol. 182, Dec. 2020, Art. no. 107516.
- [6] Y. L. Lee, D. Qin, L.-C. Wang, and G. H. Sim, "6G massive radio access networks: Key applications, requirements and challenges," *IEEE Open J. Veh. Technol.*, vol. 2, pp. 54–66, 2020.
- [7] S. Niknam, A. Roy, H. S. Dhillon, S. Singh, R. Banerji, J. H. Reed, N. Saxena, and S. Yoon, "Intelligent O-RAN for beyond 5G and 6G wireless networks," 2020, *arXiv:2005.08374*.
- [8] W. Saad, M. Bennis, and M. Chen, "A vision of 6G wireless systems: Applications, trends, technologies, and open research problems," *IEEE Netw.*, vol. 34, no. 3, pp. 134–142, 2019.
- [9] F. Hussain, S. A. Hassan, R. Hussain, and E. Hossain, "Machine learning for resource management in cellular and IoT networks: Potentials, current solutions, and open challenges," *IEEE Commun. Surveys Tuts.*, vol. 22, no. 2, pp. 1251–1275, 2nd Quart., 2020.
- [10] Z. Chen, M. Abul Masrur, and Y. L. Murphey, "Intelligent vehicle power management using machine learning and fuzzy logic," in *Proc. IEEE Int. Conf. Fuzzy Syst., IEEE World Congr. Comput. Intell.*, Jun. 2008, pp. 2351–2358.
- [11] M. Qin, Q. Yang, N. Cheng, H. Zhou, R. R. Rao, and X. Shen, "Machine learning aided context-aware self-healing management for ultra dense networks with QoS provisions," *IEEE Trans. Veh. Technol.*, vol. 67, no. 12, pp. 12339–12351, Dec. 2018.
- [12] H. Fatemidokht, M. K. Rafsanjani, B. B. Gupta, and C.-H. Hsu, "Efficient and secure routing protocol based on artificial intelligence algorithms with UAV-assisted for vehicular ad hoc networks in intelligent transportation systems," *IEEE Trans. Intell. Transp. Syst.*, vol. 22, no. 7, pp. 4757–4769, Jul. 2021.
- [13] A. Kak, "Towards 6G through SDN and NFV-based solutions for terrestrial and non-terrestrial networks," Ph.D. dissertation, Georgia Inst. Technol., Atlanta, GA, USA, 2021.
- [14] M. Mahdi Azari, S. Solanki, S. Chatzinotas, O. Kotheli, H. Sallouha, A. Colpaert, J. F. M. Montoya, S. Pollin, A. Haqiqatnejad, A. Mostaani, E. Lagunas, and B. Ottersten, "Evolution of non-terrestrial networks from 5G to 6G: A survey," 2021, *arXiv:2107.06881*.
- [15] M. Abolhasan, J. Lipman, W. Ni, and B. Hagelstein, "Software-defined wireless networking: Centralized, distributed, or hybrid?" *IEEE Netw.*, vol. 29, no. 4, pp. 32–38, Jul./Aug. 2015.
- [16] K. Benzekki, A. El Fergougui, and A. E. Elalaoui, "Software-defined networking (SDN): A survey," *Secur. Commun. Netw.*, vol. 9, no. 18, pp. 5803–5833, 2016.
- [17] A. Filali, Z. Mlika, S. Cherkaoui, and A. Kobbane, "Preemptive SDN load balancing with machine learning for delay sensitive applications," *IEEE Trans. Veh. Technol.*, vol. 69, no. 12, pp. 15947–15963, Dec. 2020.
- [18] J. Wang, Y. Miao, P. Zhou, M. Hossain, and S. M. M. Rahman, "A software defined network routing in wireless multihop network," *J. Netw. Comput. Appl.*, vol. 85, pp. 76–83, May 2016.
- [19] M. Abolhasan, M. Abdollahi, W. Ni, A. Jamalipour, N. Shariati, and J. Lipman, "A routing framework for offloading traffic from cellular networks to SDN-based multi-hop device-to-device networks," *IEEE Trans. Netw. Service Manage.*, vol. 15, no. 4, pp. 1516–1531, Dec. 2018.
- [20] K. L. K. Sudheera, M. Ma, and P. H. J. Chong, "Link stability based optimized routing framework for software defined vehicular networks," *IEEE Trans. Veh. Technol.*, vol. 68, no. 3, pp. 2934–2945, Mar. 2019.
- [21] C. Wu, S. Ohzahata, and T. Kato, "Flexible, portable, and practicable solution for routing in VANETs: A fuzzy constraint Q-learning approach," *IEEE Trans. Veh. Technol.*, vol. 62, no. 9, pp. 4251–4263, Nov. 2013.
- [22] S. Sun, Z. Cao, H. Zhu, and J. Zhao, "A survey of optimization methods from a machine learning perspective," *IEEE Trans. Cybern.*, vol. 50, no. 8, pp. 3668–3681, Nov. 2019.
- [23] S. Ali, W. Saad, N. Rajatheva, K. Chang, D. Steinbach, B. Sliwa, C. Wietfeld, K. Mei, H. Shiri, H. J. Zepernick, and T. M. C. Chu, "6G white paper on machine learning in wireless communication networks," 2020, *arXiv:2004.13875*.
- [24] D. Bega, M. Gramaglia, A. Banchs, V. Sciancalepore, and X. Costa-Perez, "A machine learning approach to 5G infrastructure market optimization," *IEEE Trans. Mobile Comput.*, vol. 19, no. 3, pp. 498–512, Mar. 2020.
- [25] Y.-R. Chen, A. Rezapour, W.-G. Tzeng, and S.-C. Tsai, "RL-routing: An SDN routing algorithm based on deep reinforcement learning," *IEEE Trans. Netw. Sci. Eng.*, vol. 7, no. 4, pp. 3185–3199, Oct. 2020.
- [26] Z. M. Zahedi, R. Akbari, M. Shokouhifar, F. Safaei, and A. Jalali, "Swarm intelligence based fuzzy routing protocol for clustered wireless sensor networks," *Expert Syst. Appl.*, vol. 55, pp. 313–328, Aug. 2016.
- [27] N. I. Abbas, M. Ilkan, and E. Ozen, "Fuzzy approach to improving route stability of the AODV routing protocol," *EURASIP J. Wireless Commun. Netw.*, vol. 2015, no. 1, pp. 1–11, Dec. 2015.
- [28] L. Zhao, Z. Bi, M. Lin, A. Hawbani, J. Shi, and Y. Guan, "An intelligent fuzzy-based routing scheme for software-defined vehicular networks," *Comput. Netw.*, vol. 187, Mar. 2021, Art. no. 107837.
- [29] H. Yao, X. Yuan, P. Zhang, J. Wang, C. Jiang, and M. Guizani, "Machine learning aided load balance routing scheme considering queue utilization," *IEEE Trans. Veh. Technol.*, vol. 68, no. 8, pp. 7987–7999, Aug. 2019.
- [30] Y. Tang, N. Cheng, W. Wu, M. Wang, Y. Dai, and X. Shen, "Delay-minimization routing for heterogeneous VANETs with machine learning based mobility prediction," *IEEE Trans. Veh. Technol.*, vol. 68, no. 4, pp. 3967–3979, Apr. 2019.
- [31] C. Ghorai, S. Shakhari, and I. Banerjee, "A SPEA-based multimetric routing protocol for intelligent transportation systems," *IEEE Trans. Intell. Transp. Syst.*, vol. 22, no. 11, pp. 6737–6747, Nov. 2021.
- [32] M. Abolhasan, T. Wysocki, and E. Dutkiewicz, "A review of routing protocols for mobile ad hoc networks," *Ad Hoc Netw.*, vol. 2, no. 1, pp. 1–22, Jan. 2004.
- [33] K. Kalkan, "SUTSEC: SDN utilized trust based secure clustering in IoT," *Comput. Netw.*, vol. 178, Sep. 2020, Art. no. 107328.
- [34] T. S. J. Darwish, K. A. Bakar, and K. Haseeb, "Reliable intersection-based traffic aware routing protocol for urban areas vehicular ad hoc networks," *IEEE Intell. Transp. Syst. Mag.*, vol. 10, no. 1, pp. 60–73, Jan. 2018.
- [35] C. Wang, *A Study of Membership Functions on Mamdani-Type Fuzzy Inference System for Industrial Decision-Making*. Bethlehem, PA, USA: Lehigh Univ., 2015.
- [36] S. A. M. Ghaleb and V. Vasanthi, "Energy efficient multipath routing using multi-objective grey wolf optimizer based dynamic source routing algorithm for manet," *Int. J. Adv. Sci. Technol.*, vol. 29, no. 3, pp. 6096–6117, 2020.
- [37] H. T. Friis, "A note on a simple transmission formula," *Proc. IRE*, vol. 34, no. 5, pp. 254–256, May 1946.



SEPEHR ASHTARI (Graduate Student Member, IEEE) received the B.S. degree (Hons.) in electrical and electronic engineering from Eastern Mediterranean University (EMU), North Cyprus, Turkey, in 2016, and the M.S. degree (Hons.) in telecommunication engineering from the University of New South Wales (UNSW), Sydney, Australia, in 2019. He is currently pursuing the Ph.D. degree in telecommunication and information technology with the University of Technology

(UTS), Sydney.

From 2015 to 2016, he was a Research Assistant with the Electrical and Electronic Engineering Department, North Cyprus. He has worked as a Research Fellow with The Commonwealth Scientific and Industrial Research Organization (CSIRO) on several wireless communication projects. His research interests include improving wireless cellular communication, routing protocols, software or knowledge-based networking, 5G resource allocation, and machine learning optimization in wireless networks.

Mr. Ashtari's awards and honors include the Fellowship of Excellence from the Department of Electrical and Electronic Engineering, and the Fellowship Award from the UTS Faculty of Engineering and IT.



MEHRAN ABOLHASAN (Senior Member, IEEE) is currently an Associate Professor and the Deputy Head of the School of Electrical and Data Engineering, University of Technology Sydney. He has over 20 years of experience in research and development and serving in research leadership roles. Some of these previous roles include serving as the Director of research programs with the Faculty of Engineering and IT, and the Laboratory Director of the Telecommunication and IT Research Institute, University of Wollongong. He has authored over 160 international publications and has won over four million dollars in research funding. He won a number of major research project grants, including the ARC Discovery Project, ARC Linkage Project, and a number of CRC and other government and industry-based grants. He currently leads the Software-Defined Networks Laboratory, UTS. His current research interests include software defined networking, the IoT, wireless mesh, wireless body area networks, cooperative networks, 5G networks, and sensor networks.



JUSTIN LIPMAN (Senior Member, IEEE) received the Ph.D. degree in telecommunications engineering from the University of Wollongong, Australia, in 2004. He is currently an Industry Associate Professor with the University of Technology Sydney (UTS) and a Visiting Associate Professor with the Graduate School of Engineering, Hokkaido University. He is also the Director of Research Translation with the Faculty of Engineering and IT and the Director of the RF Communications Technologies (RFCT) Laboratory, where he leads industry engagement in RF technologies, the Internet of Things, tactile internet, and software defined communication. He serves as Committee Member for Standards Australia contributing to International IoT Standards and Digital Twins. Prior to joining UTS, he was based in Shanghai, China, and held a number of a senior management and the technical leadership roles at Intel and Alcatel driving research and innovation, product development, architecture, and IP generation. His research interests include all “things” adaptive, connected, distributed, and ubiquitous.



NEGIN SHARIATI (Senior Member, IEEE) received the Ph.D. degree in electrical, electronic and communication technologies from the Royal Melbourne Institute of Technology (RMIT), Australia, in 2016. She is currently a Senior Lecturer with the School of Electrical and Data Engineering, Faculty of Engineering and IT, University of Technology Sydney (UTS), Australia. She established the state of the art RF and Communication Technologies (RFCT) Research Laboratory, UTS, in 2018, where she is currently the Co-Director and leads research and development in RF-electronics, sustainable sensing, low-power Internet of Things, and energy harvesting. She leads the Sensing Innovations Constellation at Food Agility Corporative Research Centre (CRC), enabling new innovations in agriculture technologies by focusing on three key interrelated streams, energy, sensing, and connectivity. Since 2018, she has been a Senior Lecturer with Hokkaido University, externally engaging with research and teaching activities in Japan. She attracted over \$850K worth of research funding across a number of CRC and industry projects, where she has taken the lead CI role and also contributed as a member of the CI Team. She worked in industry as an Electrical-Electronic Engineer, from 2009 to 2012. Her research interests include microwave circuits and systems, RF energy harvesting, low-power IoT, simultaneous wireless information and power transfer, wireless networks, AgTech, and renewable energy systems.



WEI NI (Senior Member, IEEE) received the B.E. and Ph.D. degrees in electronic engineering from Fudan University, Shanghai, China, in 2000 and 2005, respectively. He is currently the Group Leader and the Principal Research Scientist at CSIRO, Sydney, Australia, an Adjunct Professor with the University of Technology Sydney, and an Honorary Professor at Macquarie University. He was a Postdoctoral Research Fellow at Shanghai Jiao Tong University, from 2005 to 2008, the Deputy Project Manager at the Bell Laboratories, Alcatel/Alcatel-Lucent, from 2005 to 2008, and a Senior Researcher at Devices Research and Development, Nokia, from 2008 to 2009. His research interests include machine learning, stochastic optimization, online learning, and their applications to system efficiency and integrity. He has been the Chair of IEEE Vehicular Technology Society (VTS) New South Wales (NSW) Chapter, since 2020, and an Editor of IEEE TRANSACTIONS ON WIRELESS COMMUNICATIONS, since 2018. He served first as the Secretary and then the Vice-Chair of IEEE NSW VTS Chapter, from 2015 to 2019, the Track Chair for VTC-Spring 2017, the Track Co-Chair for IEEE VTC-Spring 2016, the Publication Chair for BodyNet 2015, and the Student Travel Grant Chair for WPMC 2014.



ABBAS JAMALIPOUR (Fellow, IEEE) received the Ph.D. degree in electrical engineering from Nagoya University, Nagoya, Japan, in 1996. He is currently a Professor in ubiquitous mobile networking with The University of Sydney. Since January 2022, he has been the Editor-in-Chief of the IEEE TRANSACTIONS ON VEHICULAR TECHNOLOGY. He has authored nine technical books, 11 book chapters, over 550 technical papers, and five patents, all in the area of wireless communications and networking. He was a recipient of the number of prestigious awards, such as the 2019 IEEE ComSoc Distinguished Technical Achievement Award in Green Communications, the 2016 IEEE ComSoc Distinguished Technical Achievement Award in Communications Switching and Routing, the 2010 IEEE ComSoc Harold Sobol Award, the 2006 IEEE ComSoc Best Tutorial Paper Award, and over 15 Best Paper Awards. He was the President of the IEEE Vehicular Technology Society (2020–2021). Previously, he was the Executive Vice-President and the Editor-in-Chief of VTS Mobile World and has been an Elected Member of the Board of Governors of the IEEE Vehicular Technology Society, since 2014. He was the Editor-in-Chief of the IEEE WIRELESS COMMUNICATIONS, the Vice President of Conferences, and a member of Board of Governors of the IEEE Communications Society. He sits on the Editorial Board of the IEEE ACCESS and several other journals and is a member of Advisory Board of IEEE INTERNET OF THINGS JOURNAL. He has been the General Chair or the Technical Program Chair for several prestigious conferences, including IEEE ICC, GLOBECOM, WCNC, and PIMRC. He is a fellow of the Institute of Electrical, Information, and Communication Engineers (IEICE) and the Institution of Engineers Australia, an ACM Professional Member, and an IEEE Distinguished Speaker.

• • •